

Article

Microelongated Thermo-Elastodiffusive Waves of Excited Semiconductor Material under Laser Pulses Impact

Ismail M. Tayel ¹, Kh. Lotfy ^{2,3,*}, Alaa A. El-Bary ^{4,5}, Jawdat Alebraheem ¹ and Mogtaba A. Y. Mohammed ¹

¹ Department of Mathematics, College of Science Al-Zulfi, Majmaah University, Al Majmaah 11952, Saudi Arabia; i.tayel@mu.edu.sa (I.M.T.)

² Department of Mathematics, Faculty of Science, Zagazig University, Zagazig P.O. Box 44519, Egypt

³ Department of Mathematics, Faculty of Science, Taibah University, Madinah 42353, Saudi Arabia

⁴ Arab Academy for Science, Technology and Maritime Transport, Alexandria P.O. Box 1029, Egypt

⁵ National Committee for Mathematics, Academy of Scientific Research and Technology, Cairo 4262104, Egypt

* Correspondence: khlotfy@zu.edu.eg

Abstract: The current study focuses on one-dimensional (1D) deformation in an excited microelongated semiconductor medium impacted by optoelectronics with exponential laser-pulsed heat. Diffusion effect is considered in a photothermal problem of a semiconducting media. Microelongated optoelectronics and a broad variety of concepts have been introduced. Appropriate solutions to a set of microelongated photothermal diffusion differential equations have been found. The homogeneous (thermal and mechanical) and isotropic characteristics of the medium are thought to be in the x -direction, including coupled diffusion equations. The linear photo-thermoelasticity (PTE) theory of semiconductors is used to describe thermo-elastodiffusive waves. As a case study, the developed theoretical framework may be used to explore the microelongation-photo-thermoelastic problem in a semiconductor medium caused by the laser pulse. The analytical linear solutions for the main quantities during thermoelastic (TD) and electronic (ED) deformation are obtained using Laplace transforms for dimensionless quantities. To obtain exact expressions of the important physical variables according to certain boundary surface conditions, numerical approximations solutions of the fundamental relevant relations are performed in the Laplace inverse time domain. To describe the wave propagation of the physical fields graphically, the computational results for silicon (Si) semiconductor material are derived using several cases of thermal memory and microelongation factors.

Keywords: electrons; photoexcited; microelongation; thermo-elastic waves; laser pulse; semiconductors

MSC: 74A15



Citation: Tayel, I.M.; Lotfy, K.; El-Bary, A.A.; Alebraheem, J.; Mohammed, M.A.Y. Microelongated Thermo-Elastodiffusive Waves of Excited Semiconductor Material under Laser Pulses Impact. *Mathematics* **2023**, *11*, 1627. <https://doi.org/10.3390/math11071627>

Academic Editor: Hovik Matevossian

Received: 26 February 2023

Revised: 18 March 2023

Accepted: 22 March 2023

Published: 28 March 2023



Copyright: © 2023 by the authors. Licensee MDPI, Basel, Switzerland. This article is an open access article distributed under the terms and conditions of the Creative Commons Attribution (CC BY) license (<https://creativecommons.org/licenses/by/4.0/>).

1. Introduction

A substance known as a semiconductor material has electrical conductivity attributes that fall in between those of a conductor and those of non-conductor or insulator materials. This suggests that semiconductors may change their behavior from conducting to insulating depending on the external environment. As the temperature increases, a semiconductor's internal resistance gradually decreases, enabling a current to pass through it. The most well-known, pure semiconductor is silicon, whereas gallium arsenide is a compound semiconductor element. In recent years, the scientific world has been more interested in semiconductor gain processes on ultrafast time scales. To investigate how semiconductor laser amplifiers react to ultrashort (picosecond or shorter time scales) light pulses in this region, some experimental approaches have been carried out. Empirical testing has shown the complexity of gain, measured along the timeframe in the order of picoseconds. The idea that this kind of gain response is caused by unusual behavior of the carrier ensemble on short time scales; notably, the conduction of dynamic carrier heating is supported by mathematical calculations [1]. The process of electronic deformation (ED) occurs when the

electrons go to the surface after being tremendously excited. On the other hand, the increase in temperature causes the inner particles to vibrate and collide, allowing thermoelastic deformation (TE) to emerge. In this situation, semiconductor materials may be studied as elastic materials. These materials may be studied using the so-called photo-thermoelasticity theory during ED and TE deformation processes [2]. In light of these deformations, it is necessary to take into account the microinertia process of the material's microelements (ED and TD). The behavior of semiconductor materials with changing internal structures is insufficiently explained by classical theories [3]. In contemporary science, the surface deformation of a material is now dominated by laser heating. An extremely adaptable tool for altering the surfaces of materials is the laser. When the laser's intensity is extremely high, it interacts with the surface of the material and causes absorption there.

Attempts to predict the behavior of materials with internal structures using just the classical theory have shown to be inadequate. Eringen and Suhubi [4,5] have suggested a nonlinear theory for microelastic solids. Eringen [6–8] devised the linear theory of micropolar elasticity, which accounts for the fact that material particles in solids may undergo both macro- and micro-rotations. Axial stretch was considered in Eringen's [9] model of a micropolar elastic solid. The micropolar hypothesis was expanded by many writers to include thermal effects [10–13]. Both the idea of temperature rate-dependent thermoelasticity and the theory of Lord and Shulman [14] are significant examples of generalized thermoelasticity. In a study of the thermodynamics of thermoelastic substances, Muller [15] proposed an entropy production inequality, which restricts a specific class of constitutive equations. A generalization of this inequality was introduced by Green and Laws [16]. Green and Lindsay [17] established an alternate representation of these constitutive equations. All the equations of the coupled theory are modified by these two constants, which were created independently and explicitly and act as relaxation times [12]. Nevertheless, Shaw and Othman [18] investigated specific issues in the thermoelasticity theory by means of a conformable fractional differential equation. Rayleigh and Reflection wave propagation in a nonlocal rotating isotropic piezo-thermoelastic material with fractional derivatives was investigated by Lata et al. [19–23].

Around the beginning of the twentieth century, studies into semiconductor properties were beginning to be conducted. Due to scientific and industrial advances, semiconductors had extensive applications in the 20th century, being incorporated into anything from solar cells that produce renewable energy to electrical circuits in medical equipment. Maruszewski [24,25] introduced new theoretical models that take into account the interplay of the elastic, thermal, and charge carrier fields in elastic semiconductors. The thermal diffusivity of semiconductors during heat and mass transport processes has recently been studied based on the overlap between thermal, elastic, and plasma waves [26,27]. The photothermal (PT) technique is used in contemporary research on delicate photoacoustic processes in semiconductor materials [28]. Both TE and ED deformation are required by the PT process, which analyses semiconductors' physical characteristics. The effects of a laser beam, electromagnetic radiation, and acoustic waves on a semiconductor material were investigated [29]. The photo-thermoelasticity theory was used by several authors to study a variety of topics about elastic semiconductor materials [30–32]. The absorbed optical energy on the free surface of homogeneous and non-homogeneous semiconductor materials was examined when thermal conductivity varied during PT transport activities [33–37]. Khamis et al. [38] studied the semiconductor medium under the impact of thermal piezoelectricity in the context of photo-thermal excitation. Mahdy et al. [39,40] used the time-fractional heat order and Thomson effects under the impact of pulse heat flux to investigate the magneto-photothermal semiconductor medium during variable thermal conductivity. In all of the aforementioned studies, the interaction between electrons and holes was ignored while they were examining semiconductors using PT theory. However, the effect of microelongation under the effect of laser pulses has been ignored when there was no heat source. The excited electrons with holes were found to be dispersed toward the semiconductor's surface and

move about, creating an electron cloud known as carrier density and hole charge in studies on the characteristics of semiconductors (plasma).

The main objective of this work is to examine the effects of electron diffusion in the presence of microelongation parameters. The homogeneous, isotropic, microelongated semiconductor medium is used to analyze the propagation of elasto-thermodiffusive waves during photo-generated excitation. In this paper, we use the photo-thermoelasticity theory to the study of laser-induced thermo-elastodiffusive waves in a semiconductor medium. A new model for one-dimensional deformation processes is developed using the microelongated semiconductor in accordance with the microinertia of medium. A completely new mathematical photo-thermoelasticity model is developed, including elongation in 1D deformation and dimensionless quantities. Under the appropriate conditions, Laplace transforms for the partial differential governing equation are applied analytically. Mathematically, the reverse of the Laplace transform is numerically utilized to provide the complete solutions of the main variables in this problem. Finally, by presenting the results of the physical field quantities graphically, analytical verification can be provided. The impacts of microelongation and laser pulses factor are studied, as well as the thermal memory of silicon medium. Graphical representations of the numerical findings have been made and are discussed.

2. Governing Equation

The Cartesian coordinate is utilized in 1D deformation at reference temperature T_0 , in which case all field variables are independent of the y and z coordinates. In the linear theory of photo-thermoelasticity of microelongated semiconductors, the governing field equations in 1D for temperature distribution $T(x, t)$, the microelongational function $\varphi(x, t)$, displacement $u(x, t)$, $H(x, t)$ and electron diffusion field (carrier density) $N(x, t)$ depend on the time t and the x -axis in accordance with the semiconductor’s electric neutrality. The constitutive equations for microelongated semiconductor photo-thermoelastic media are presented in the general form of tensors [2]:

$$\left. \begin{aligned} \sigma_{iI} &= (\lambda_o \varphi + \lambda u_{r,r}) \delta_{iI} + 2\mu u_{i,i} - \delta_{iI} \delta_h H - \hat{\gamma} (1 + v_o \frac{\partial}{\partial t}) T \delta_{iI} - ((3\lambda + 2\mu) d_n N) \delta_{iI}, \\ m_i &= a_o \varphi_{,i}, \\ s - \sigma &= \lambda_o u_{i,i} - \beta_1 (1 + \tau_\theta \frac{\partial}{\partial t}) T + -((3\lambda + 2\mu) d_n N) \delta_{2i} - \delta_{2i} \delta_h H + \lambda_1 \varphi. \end{aligned} \right\}, \quad (1)$$

When the body forces electro-magnetic pressure and heat sources are absent, according to the microelongated photo-thermoelastic theory, the main equations may be found in 1D [9].

$$\rho \frac{\partial^2 u}{\partial t^2} = (2\mu + \lambda) \frac{\partial^2 u}{\partial x^2} - \gamma (1 + \tau_\theta \frac{\partial}{\partial t}) \frac{\partial T}{\partial x} + \lambda_o \frac{\partial \varphi}{\partial x} - \delta_n \frac{\partial N}{\partial x} - \delta_h \frac{\partial H}{\partial x}, \quad (2)$$

$$\left. \begin{aligned} K(1 + \tau_\theta \frac{\partial}{\partial t}) \frac{\partial^2 T}{\partial x^2} + m_{nq} \frac{\partial^2 N}{\partial x^2} + m_{hq} \frac{\partial^2 H}{\partial x^2} - \rho (a_1^n \frac{\partial N}{\partial t} + a_1^h \frac{\partial H}{\partial t}) - \\ (1 + \tau_q \frac{\partial}{\partial t}) \left[\rho C_e \frac{\partial T}{\partial t} + \rho T_0 \alpha_n \frac{\partial N}{\partial t} + \rho T_0 \alpha_h \frac{\partial H}{\partial t} + T_0 \gamma \frac{\partial}{\partial x} \frac{\partial u}{\partial t} \right] - \\ \left[\frac{\rho a_1^n}{t^n} N + \frac{\rho a_1^h}{t^h} H \right] = \hat{\gamma}_1 T_o \frac{\partial \varphi}{\partial t} \end{aligned} \right\}, \quad (3)$$

$$\left. \begin{aligned} m_{qn} \frac{\partial^2 T}{\partial x^2} + D_n \rho \frac{\partial^2 N}{\partial x^2} - \rho (1 - a_2^n T_0 \alpha_n + t^n \frac{\partial}{\partial t}) \frac{\partial N}{\partial t} \\ - a_2^n \left[\rho C_e \frac{\partial T}{\partial t} + \rho T_0 \alpha_n \frac{\partial H}{\partial t} + T_0 \gamma \frac{\partial}{\partial x} \frac{\partial u}{\partial t} \right] = - \frac{\rho}{t^n} (1 + t^n \frac{\partial}{\partial t}) N \end{aligned} \right\}, \quad (4)$$

$$\left. \begin{aligned} m_{qh} \frac{\partial^2 T}{\partial x^2} + D_h \rho \frac{\partial^2 H}{\partial x^2} - \rho (1 - a_2^h T_0 \alpha_h + t^h \frac{\partial}{\partial t}) \frac{\partial H}{\partial t} - \\ a_2^h \left[\rho C_e \frac{\partial T}{\partial t} + \rho T_0 \alpha_n \frac{\partial N}{\partial t} + T_0 \gamma \frac{\partial}{\partial t} \frac{\partial u}{\partial x} \right] = - \frac{\rho}{t^h} (1 + t^h \frac{\partial}{\partial t}) H \end{aligned} \right\}, \quad (5)$$

$$\alpha_o \frac{\partial^2 \varphi}{\partial x^2} - \lambda_1 \varphi - \lambda_o \frac{\partial u}{\partial x} + \gamma_1 \left(1 + \tau_\theta \frac{\partial}{\partial t} \right) T = \frac{1}{2} j \rho \frac{\partial^2 \varphi}{\partial t^2}, \quad (6)$$

where δ_h is the elastic-diffusive parameter of holes, k expresses the diffusivity, D_h is the coefficients of diffusion for the holes, $\gamma_1 = (3\lambda + 2\mu)\alpha_\theta$, α_θ is the microelongational thermal expansions coefficient, t^h is the thermal memories of holes, and α_h is the thermos-diffusive constants of the holes. The other notations correspond as: $a_1^n = \frac{a_{Qn}}{a_Q}$, $a_1^h = \frac{a_{Qh}}{a_Q}$, $a_2^n = \frac{a_{Qn}}{a_n}$ and $a_2^h = \frac{a_{Qh}}{a_h}$.

For the effects of the electron and hole carrier field in 1D, the microelongated constitutive equation is as follows [41]:

$$\sigma_{xx} = (2\mu + \lambda) \frac{\partial u}{\partial x} - (\gamma(1 + \tau_\theta \frac{\partial}{\partial t})T + \delta_n N) - \delta_h H + \lambda_1 \varphi = \sigma. \tag{7}$$

The main equations shown in [36–40] may be simplified further by transforming them using the dimensionless values listed below:

$$\left. \begin{aligned} (x', u') &= \frac{\omega^*(x, u)}{C_T}, (t', \tau'_q, \tau'_\theta, t^{n'}, t^{h'}, t_1^{n'}, t_1^{h'}) = \omega^*(t, \tau_q, \tau_\theta, t^n, t^h, t_1^n, t_1^h), C_L^2 = \frac{\mu}{\rho}, \\ \beta^2 &= \frac{C_T^2}{C_L^2}, k = \frac{K}{\rho C_e}, \sigma'_{ij} = \frac{\sigma_{ij}}{2\mu + \lambda}, N' = \frac{\delta_n(N)}{2\mu + \lambda}, C_T^2 = \frac{2\mu + \lambda}{\rho}, \bar{\varphi} = \frac{\rho C_T^2}{T_0 \hat{\gamma}} \varphi, \\ \omega^* &= \frac{C_e(\lambda + 2\mu)}{K}, (\bar{\delta}_n, \bar{\delta}_h) = \frac{(\delta_n n_0, \delta_h h_0)}{\gamma T_0}, T' = \frac{\gamma T}{2\mu + \lambda}, H' = \frac{\delta_n(H)}{2\mu + \lambda}. \end{aligned} \right\} \tag{8}$$

When Equation (8) is used in combination with Equations (2)–(7), the dashes are omitted for convenience, resulting in:

$$\left\{ \frac{\partial^2}{\partial x^2} - \frac{\partial^2}{\partial t^2} \right\} u - (1 + \tau_\theta \frac{\partial}{\partial t}) \frac{\partial T}{\partial x} - \frac{\partial N}{\partial x} + a_1 \frac{\partial \varphi}{\partial x} - \alpha_{21} \frac{\partial H}{\partial x} = 0, \tag{9}$$

$$\left\{ \begin{aligned} & \left((1 + \tau_\theta \frac{\partial}{\partial t}) \frac{\partial^2}{\partial x^2} - (1 + \tau_q \frac{\partial}{\partial t}) \frac{\partial}{\partial t} \right) T + \left(\alpha_1 \frac{\partial^2}{\partial x^2} - \alpha_2 (1 + \tau_q \frac{\partial}{\partial t}) - \alpha_3 \frac{\partial}{\partial t} - \alpha_4 \right) N + \\ & \left(\alpha_5 \frac{\partial^2}{\partial x^2} - (1 + \tau_\alpha \frac{\partial}{\partial t}) \alpha_6 - \alpha_7 \right) H - \varepsilon_1 (1 + \tau_q \frac{\partial}{\partial t}) \frac{\partial}{\partial t} \left(\frac{\partial u}{\partial x} \right) - \zeta \frac{\partial \varphi}{\partial t} = 0 \end{aligned} \right\}, \tag{10}$$

$$\left\{ \begin{aligned} & \left\{ \frac{\partial^2}{\partial x^2} - \alpha_8 \frac{\partial}{\partial t} \right\} T + \left\{ \alpha_9 \frac{\partial^2}{\partial x^2} - (\alpha_{10} + t^n \frac{\partial}{\partial t}) \alpha_{11} + (1 + t^n \frac{\partial}{\partial t}) \frac{\alpha_{11}}{t^n} \right\} N - \\ & \alpha_{12} \frac{\partial H}{\partial t} - \alpha_{13} \frac{\partial}{\partial x} \frac{\partial u}{\partial t} = 0 \end{aligned} \right\}, \tag{11}$$

$$\left\{ \begin{aligned} & \left\{ \frac{\partial^2}{\partial x^2} - \alpha_{18} \frac{\partial}{\partial t} \right\} T + \left\{ \alpha_{14} \frac{\partial^2}{\partial x^2} - (\alpha_{15} + t^h \frac{\partial}{\partial t}) \alpha_{16} \frac{\partial}{\partial t} + (1 + t^h \frac{\partial}{\partial t}) \alpha_{17} \right\} H - \\ & \alpha_{19} \frac{\partial N}{\partial t} - \alpha_{20} \frac{\partial}{\partial t} \frac{\partial u}{\partial x} = 0 \end{aligned} \right\}, \tag{12}$$

$$\left(\frac{\partial^2}{\partial x^2} - C_3 - C_4 \frac{\partial^2}{\partial t^2} \right) \varphi - C_5 \frac{\partial u}{\partial x} + C_6 (1 + \tau_\theta \frac{\partial}{\partial t}) T = 0 \tag{13}$$

$$\sigma_{xx} = \left(\frac{\partial u}{\partial x} - (1 + \tau_\theta \frac{\partial}{\partial t}) T + N \right) + a_1 \varphi - H = \sigma. \tag{14}$$

where

$$\begin{aligned} \alpha_1 &= \frac{m_{nq} \alpha_t}{d_n K}, \alpha_2 = \frac{T_0 \alpha_n}{C_e}, \alpha_3 = \frac{a_1^n}{C_e}, \alpha_4 = \frac{a_1^n \gamma}{C_e \tau^n (2\mu + \lambda)}, \alpha_5 = \frac{\gamma m_{hq} h_0}{(2\mu + \lambda) K}, \alpha_6 = \frac{T_0 \alpha_h K h_0}{C_e}, \\ \alpha_7 &= \frac{a_1^h \gamma \omega^*}{t^h K}, \alpha_8 = \frac{a_2^n K}{m_{qn}}, \alpha_9 = \frac{D_n \rho \alpha_t}{m_{qn} d_n}, \alpha_{10} = 1 - a_2^n T_0 \alpha_n, \alpha_{11} = \frac{\alpha_t K}{m_{qn} d_n C_e}, \alpha_{12} = \frac{a_2^n \gamma h_0 \alpha_h \omega^*}{m_{qn}}, \\ \alpha_{13} &= \frac{a_2^n \gamma^2 T_0 \omega^*}{\rho m_{qn}}, \alpha_{14} = \frac{D_n h_0 \gamma}{C_T^2 m_{qh}}, \alpha_{15} = 1 - a_2^h T_0 \alpha_n, \alpha_{16} = \frac{\gamma h_0 \omega^*}{m_{qh}}, \alpha_{17} = \frac{\gamma h_0 \omega^*}{m_{qh} \tau_1^h}, \alpha_{18} = a_2^h \frac{K}{m_{qh}}, \\ \alpha_{19} &= \frac{a_2^h \gamma T_0 \alpha_n (2\mu + \lambda) \omega^*}{m_{qh} \delta_n}, \alpha_{20} = \frac{a_2^h \gamma^2 T_0 \omega^*}{m_{qh} \rho}, \alpha_{21} = \frac{\delta_h}{(2\mu + \lambda)}, \varepsilon_1 = \frac{T_0 \gamma^2 \omega^*}{\rho K}, a_1 = \frac{\lambda_0}{\rho C_T^2}, \zeta = \frac{\hat{\gamma}_1 \hat{\gamma} T_0}{K \rho}, \\ C_3 &= \frac{\lambda_1 \omega^{*2}}{\alpha_0 C_T^2}, C_4 = \frac{\rho j \omega^{*4}}{\alpha_0 C_2^2}, C_5 = \frac{\lambda_0 \omega^{*2}}{\alpha_0 C_T^2}, C_6 = \frac{\hat{\gamma}_1 \rho \omega^{*2} T_0}{\hat{\gamma} \alpha_0}. \end{aligned}$$

The following initial conditions, which may be expressed as follows, should be taken into account for this problem:

$$\begin{aligned}
 u(x, t)|_{t=0} &= \left. \frac{\partial u(x, t)}{\partial t} \right|_{t=0} = 0, \quad T(x, t)|_{t=0} = \left. \frac{\partial T(x, t)}{\partial t} \right|_{t=0} = 0, \quad N(x, t)|_{t=0} = \left. \frac{\partial N(x, t)}{\partial t} \right|_{t=0} = 0, \\
 \varphi(x, t)|_{t=0} &= \left. \frac{\partial \varphi(x, t)}{\partial t} \right|_{t=0} = 0, \quad H(x, t)|_{t=0} = \left. \frac{\partial H(x, t)}{\partial t} \right|_{t=0} = 0
 \end{aligned}
 \tag{15}$$

3. Analytical Solution Procedure

The partial differential equations are transformed into ordinary differential equations in the time–space domain using the above conditions provided (ODE). These methods, with Equation (15), may be used to build function $\Delta(x, t)$ according to the Laplace transform:

$$L(\Delta(x, t)) = \bar{\Delta}(x, s) = \int_0^\infty \Delta(x, t) \exp(-st) dt.
 \tag{16}$$

The following equations may be derived from the Laplace transform Equation (16):

$$(D^2 - s^2)\bar{u} - q_{14}D\bar{T} - D\bar{N} - a_1D\bar{\varphi} - \alpha_{21}\bar{H} = 0,
 \tag{17}$$

$$(q_1 D^2 - q_2)\bar{T} + (\alpha_1 D^2 - q_3)\bar{N} + (\alpha_5 D^2 - q_4)\bar{H} - q_5 D\bar{u} - s\zeta\bar{\varphi} = 0,
 \tag{18}$$

$$(D^2 - q_7)\bar{T} + (\alpha_9 D^2 - q_6)\bar{N} - q_8\bar{H} - q_9 D\bar{u} = 0,
 \tag{19}$$

$$(D^2 - q_{10})\bar{T} + (\alpha_{14} D^2 - q_{11})\bar{H} - q_{12}\bar{N} - q_{13} D\bar{u} = 0,
 \tag{20}$$

$$(D^2 - C_7)\varphi - C_5 D u + C_8 T = 0,
 \tag{21}$$

$$\bar{\sigma} = D\bar{u} - (1 + s\tau_\theta)(\bar{T} + \bar{N}) + a_1\bar{\varphi} - \bar{H}.
 \tag{22}$$

where

$$\begin{aligned}
 D &= \frac{d}{dx}, \quad q_1 = (1 + \tau_\theta s), \quad q_2 = (1 + \tau_q s) s, \quad q_3 = (\alpha_2(1 + \tau_q s) + \alpha_3 s + \alpha_4), \quad q_4 = (1 + \tau_q s)\alpha_6 + \alpha_7 \\
 q_5 &= (1 + \tau_q s)\varepsilon_1 s, \quad q_6 = (\alpha_{10} + t^n s)\alpha_{11} - (1 + t^n s)\frac{\alpha_{11}}{t^n}, \quad q_7 = \alpha_8 s, \quad q_8 = \alpha_{12} s, \quad C_7 = C_3 + C_4 s^2, \\
 q_9 &= \alpha_{13} s, \quad q_{10} = \alpha_{18} s, \quad q_{11} = (\alpha_{15} + t^h s)\alpha_{16} s - (1 + t^h s)\alpha_{17}, \quad q_{12} = \alpha_{19} s, \quad q_{13} = \alpha_{20} s, \quad C_8 = C_6 q_1.
 \end{aligned}$$

The following differential equation may be obtained by using the process of elimination between quantities $\bar{T}, \bar{u}, \bar{H}, \bar{N}$ and $\bar{\varphi}$ in the preceding equation:

$$(D^{10} - \eta_1 D^8 + \eta_2 D^6 - \eta_3 D^4 + \eta_4 D^2 + \eta_5) \{\bar{\varphi}, \bar{T}, \bar{N}, \bar{H}, \bar{u}\} = 0
 \tag{23}$$

where

$$\begin{aligned}
 \eta_1 &= \frac{-1}{\alpha_1} \{ \beta\alpha_9 q_1 - s^2\alpha_1 + \alpha_1 q_1 q_{14} + \alpha_9 q_5 q_{14} - \beta\alpha_1 - \alpha_1 q_7 + \alpha_9 q_2 - q_3 - q_5 \}, \\
 \eta_2 &= \frac{1}{\alpha_1} \left\{ \begin{aligned} & -\beta s^2\alpha_9 q_1 + \beta s^2\alpha_1 - \beta\alpha_1 q_9 q_{14} - \beta\alpha_9 q_5 q_{14} + s^2\alpha_1 q_7 - s^2\alpha_9 q_2 + \beta\alpha_1 q_7 - \beta\alpha_9 q_2 - \\ & \beta q_1 q_6 + \beta q_1 q_9 + s^2 q_3 - q_3 q_9 q_{14} - q_5 q_6 q_{14} + \beta q_3 + \beta q_5 - q_2 q_6 + q_2 q_9 + q_3 q_7 + q_5 q_7 \end{aligned} \right\}, \\
 \eta_3 &= \frac{-1}{\alpha_1} \left\{ \begin{aligned} & -\beta s^2\alpha_1 q_7 + \beta s^2\alpha_9 q_2 + \beta s^2 q_1 q_6 - \beta s^2 q_3 + \beta q_3 q_9 q_{14} + \beta q_5 q_6 q_{14} + \\ & s^2 q_2 q_6 - s^2 q_3 q_7 + \beta q_2 q_6 - \beta q_2 q_9 - \beta q_3 q_7 - \beta q_5 q_7 \end{aligned} \right\}, \\
 \eta_4 &= \frac{-1}{\alpha_1} \left\{ \begin{aligned} & -\beta s^2\alpha_1 q_7 + \beta s^2\alpha_9 q_2 + \beta s^2 q_1 q_6 - q_3 q_9 q_{14} - q_5 q_6 q_{14} + \beta q_3 + \beta q_5 + \\ & -\beta s^2\alpha_9 q_1 + \beta s^2\alpha_1 - \beta\alpha_1 q_9 q_{14} - \beta\alpha_9 q_5 q_{14} + s^2\alpha_1 q_7 \end{aligned} \right\}, \\
 \eta_5 &= \frac{1}{\alpha_1} \{ -\beta s^2 q_2 q_6 + \beta s^2 q_3 q_7 \}.
 \end{aligned}$$

The differential equation’s characteristic equation is shown below:

$$(D^2 - r_1^2)(D^2 - r_2^2)(D^2 - r_3^2)(D^2 - r_4^2)(D^2 - r_5^2)\{\bar{\varphi}, \bar{T}, \bar{N}, \bar{H}, \bar{u}\} = 0 \tag{24}$$

where $r_i(i = 1, 2, 3, 4, 5)$ refers the roots of the above equation when $x \rightarrow \infty$.

The generalized linear solution of Equation (18) for the temperature is shown in the illustration below:

$$\bar{T}(x, s) = \sum_{i=1}^5 \Lambda_i(s) e^{-k_i x}. \tag{25}$$

From the other perspective, linear solutions of the other important physical quantities may be represented mathematically:

$$\bar{N}(x, s) = \sum_{i=1}^5 \Lambda'_i(s) e^{-r_i x} = \sum_{i=1}^5 H_{1i} \Lambda_i(s) e^{-r_i x}, \tag{26}$$

$$\bar{u}(x, s) = \sum_{i=1}^5 \Lambda''_i(s) e^{-r_i x} = \sum_{i=1}^5 H_{2i} \Lambda_i(s) e^{-r_i x}, \tag{27}$$

$$\bar{\varphi}(x, s) = \sum_{i=1}^5 \Lambda'''_i(s) e^{-r_i x} = \sum_{i=1}^5 H_{3i} \Lambda_i(s) e^{-r_i x}, \tag{28}$$

$$\bar{H}(x, s) = \sum_{i=1}^5 \Lambda_i'''' \exp(-r_i x) = \sum_{i=1}^5 H_{4i} \Lambda_i \exp(-r_i x), \tag{29}$$

$$\bar{\sigma}(x, s) = \sum_{i=1}^5 \Lambda_i'''' \exp(-r_i x) = \sum_{i=1}^5 H_{5i} \Lambda_i \exp(-r_i x). \tag{30}$$

where $\Lambda_i, \Lambda'_i, \Lambda''_i, \Lambda'''_i, \Lambda_i''''$ and Λ_i'''' are unknown parameters that depend on S .

$$H_{1i} = \frac{-(m_i^4 + (-s^2 + q_9 q_{14} - q_7)m_i^2 + s^2 q_7)}{(m_i^4 \alpha_9 + (-s^2 \alpha_9 - q_6 + q_9)m_i^2 + s^2 q_6)m_i^2 - \alpha_1},$$

$$H_{2i} = \frac{m_i((\alpha_9 q_{14} - 1)m_i^2 - q_6 q_{14} + q_7)}{(m_i^4 \alpha_9 + (-s^2 \alpha_9 - q_6 + q_9)m_i^2 + s^2 q_6)},$$

$$H_{3i} = \frac{-\beta}{m_i^2 - \beta}, H_{5i} = \alpha_5(m_i H_{2i} - ((1 + s\tau_\theta) + H_{1i})).$$

4. Applications

In this section of the article, we evaluate parameters Λ_i . A very little amount of heat escapes into the surrounding region as a result of pulsed laser stimulation, since temperature changes occur quickly or at least within a short period. As a consequence, pulsed laser excitation is advantageous for studies of absorption. It is also established that a range of physical reactions, some of which need energy, may take place when a laser beam impacts a solid microelongated semiconductor surface. A portion of the energy from the laser light is transformed into heat when it strikes a material. This kind of heat creation sends heat waves across the medium, which has certain impacts (e.g., photothermal effects) [41–43].

(I) When $x = 0$, the pulsing heat flow boundary condition may be represented by the thermally gradient temperature in the following ways:

$$\left. \frac{\partial T(x, t)}{\partial x} \right|_{x=0} = -q_0 \frac{t^2 e^{-\frac{t}{\tau_p}}}{16t_p^2}. \tag{31}$$

When it is applied to a thermal condition load at time of pulse heat flux t_p with constant q_0 and pulse parameter p , the Laplace transforms provide:

$$\sum_{i=1}^5 k_i \Lambda_i(s) e^{-k_i x} \Big|_{x=0} = \frac{q_0 t_p}{8(1 + p t_p)^3}. \tag{32}$$

Figure 1 illustrates the pattern that includes the temporal period of a laser pulse (exponential laser-pulsed heat):

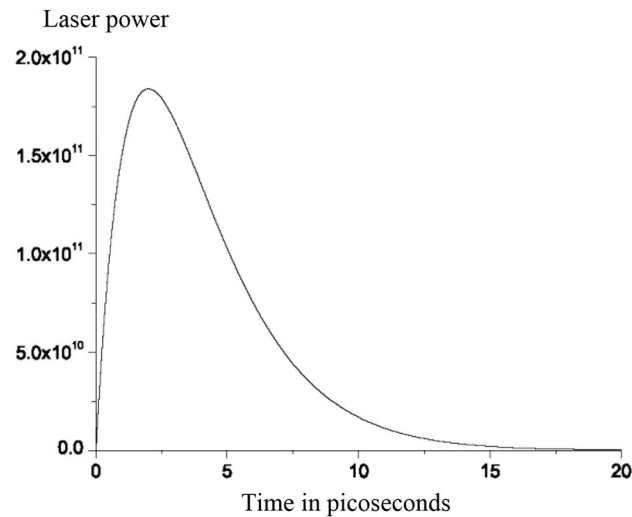


Figure 1. Temporal profile of the laser pulse.

(II) The load force \mathfrak{S} may be expressed as follows when the Laplace transform is used, and it is regarded as a mechanical condition at the boundary $x = 0$:

$$\bar{\sigma}(0, s) = \bar{\mathfrak{S}} \Rightarrow \sum_{i=1}^5 H_{4i} \Lambda_i(s) = \bar{\mathfrak{S}}. \tag{33}$$

(III) The carriers are capable of obtaining the following value on the sample’s surface, $x = 0$, as they disperse, where they have a chance of undergoing recombination. Consequently, the following equation might be used to express the carrier density boundary condition. In this, the plasma condition under the Laplace transform is derived using the carrier density diffusive and is shown as follows:

$$\bar{N}(0, s) = \frac{\hat{\lambda} n_0}{D_e} \bar{R}(s) \Rightarrow \sum_{i=1}^5 H_{1i} \Lambda_i(s) = \frac{\hat{\lambda} n_0}{s D_e}. \tag{34}$$

(IV) One may choose the microelongation condition as an elongation free on the surface $x = 0$:

$$\bar{\varphi} = 0 \Rightarrow \sum_{i=1}^5 H_{3i} \Lambda_i(s) = 0. \tag{35}$$

(V) On the other hand, the equilibrium concentration situation for the hole charge carrier field at the boundary condition may be obtained in this instance by using the Laplace transform:

$$\bar{H}(0, s) = h_0 \Rightarrow \sum_{i=1}^5 H_{4i} \Lambda_i = h_0. \tag{36}$$

where $R(s)$ is to the Heaviside unit step function and $\hat{\lambda}$ is an arbitrary parameter.

5. Inversion of the Laplace Transforms

One must invert the transforms in the physical domain to obtain the results. The complete 1D solutions for the fundamental dimensionless physical fields in the time domain may be determined by using the Laplace transform’s inverse. The Riemann-sum approximation technique and a numerical approach are used to invert the Laplace transformations. As a result, a rapid Fourier transform-based numerical inversion of the Laplace transform (NILT) approach is used [44]. For any function $\bar{\Phi}(x, s)$, it can be reversed as:

$$\Phi(x, t') = L^{-1}\{\bar{\Phi}(x, s)\} = \frac{1}{2\pi i} \int_{n-i\infty}^{n+i\infty} e^{st'} \bar{\Phi}(x, s) ds. \tag{37}$$

where $s = n + iM(n, M \in R)$. In $[0, 2t']$, the Fourier series is used to expand function $\Phi(x, t')$ as:

$$\Phi(x, t') = \frac{e^{nt'}}{t'} \left[\frac{1}{2} \bar{\Phi}(x, n) + Re \sum_{k=1}^N \bar{\Phi}(x, n + \frac{ik\pi}{t'}) (-1)^k \right]. \tag{38}$$

where $i = \sqrt{-1}$ is the imaginary unit and Re is the real part. For convergence, N is chosen freely when $nt' \approx 4.7$ [44].

6. Validation

6.1. The Microelongated Thermoelasticity Models

However, the governing Equations (2)–(6) are simplified to the generalized microelongated thermoelasticity theory when the electrons charge field (carrier density) and the holes charge field are omitted (i.e., $N = 0$ and $H = 0$). The four equations may be rewritten as follows in 1D as [7,8]:

$$K(1 + \tau_\theta \frac{\partial}{\partial t}) \frac{\partial^2 T}{\partial x^2} - (1 + \tau_q \frac{\partial}{\partial t}) \left[\rho C_e \frac{\partial T}{\partial t} + T_0 \gamma \frac{\partial}{\partial x} \frac{\partial u}{\partial t} \right] = \hat{\gamma}_1 T_0 \frac{\partial \varphi}{\partial t}, \tag{39}$$

$$\rho \frac{\partial^2 u}{\partial t^2} = (2\mu + \lambda) \frac{\partial^2 u}{\partial x^2} - \gamma(1 + \tau_\theta \frac{\partial}{\partial t}) \frac{\partial T}{\partial x} + \lambda_o \frac{\partial \varphi}{\partial x}, \tag{40}$$

$$\alpha_o \frac{\partial^2 \varphi}{\partial x^2} - \lambda_1 \varphi - \lambda_o \frac{\partial u}{\partial x} + \gamma \left(1 + \tau_\theta \frac{\partial}{\partial t} \right) T = \frac{1}{2} j \rho \frac{\partial^2 \varphi}{\partial t^2}, \tag{41}$$

$$(2\mu + \lambda) \frac{\partial u}{\partial x} - \gamma(1 + \tau_\theta \frac{\partial}{\partial t}) T + \lambda_1 \varphi = \sigma. \tag{42}$$

The dual-phase lag (DPL) when $0 \leq \tau_\theta < \tau_q$ is obtained. The Lord and Şulman (LS) model can be observed when $\tau_\theta = 0$ and $0 < \tau_q$. Finally, the coupled thermos-elasticity (CT) model is introduced when $\tau_\theta = \tau_q = 0.0$.

6.2. The Influence of Microelongation Parameters

When the microelongation parameters are ignored ($\alpha_o = \lambda_o = \lambda_1 = 0$), the set of equations describes the case of the generalized photo-thermoelasticity theory when one is taking into consideration the interaction between the elastic, thermal, and electronic waves, and holes [45–47].

6.3. The Laser Pulses Impact

The effect of the exponential laser-pulsed heat is shown by the preceding basic boundary condition (I). When the power intensity of the effect of the laser pulses is disregarded, the model under examination transforms into a model of the photo-thermoelasticity theory with a holes effect under the impact of microelongation parameters [45].

7. Numerical Results and Discussion

The authors validated the accuracy of the theoretical and analytical conclusions that were obtained and compared them to previous achievements. The numerical simulations of wave propagation in the significant physical fields are discussed in this section. The elastic wave (displacement), plasma wave (electron diffusion), mechanical wave (stress), holes charge, and thermal wave that are created for a short time may all be graphically represented. Utilizing the input parameters in the SI unit of the microelongated semiconductor silicon (Si) material, the Matlab (2022a) software of the authors' computer is used to graph the distribution of the main wave distributions. The following physical constants for Si are listed in Table 1 [46,47]:

Table 1. The SI units of the physical constants for Si medium.

Unit	Symbol	Value
N/m ²	λ	6.4×10^{10}
	μ	6.5×10^{10}
kg/m ³	ρ	2330
K	T_0	800
sec (s)	τ	5×10^{-5}
K ⁻¹	α_t	4.14×10^{-6}
Wm ⁻¹ K ⁻¹	K	150
J/(kg K)	C_e	695
m/s	\tilde{s}	2
	m_{qn}	1.4×10^{-5}
	m_{nq}	1.4×10^{-5}
	m_{qh}	-0.004×10^{-6}
vk ⁻¹	m_{hq}	-0.004×10^{-6}
	p	10^{11}
J · m ⁻²	p	10^{11}
m ² s ⁻¹	D_n	0.35×10^{-2}
m ² s ⁻¹	D_h	0.125×10^{-2}
m ² /s	α_n	1×10^{-2}
m ² /s	α_h	5×10^{-3}
ps	t_p	4
Constants	q_0	3
	\Im	2
J · m ⁻²	p	10^{11}
m ²	j	0.2×10^{-19}
Nm ⁻²	λ_0	0.5×10^{10}
Nm ⁻²	λ_1	0.5×10^{10}
Nm ⁻²	k	10^{10}
K ⁻¹	α_θ	0.017×10^{-3}
Nm ⁻²	α_0	0.779×10^{-9}

7.1. The Photo-Thermoelasticity Models

According to models based on the theory of microelongated photo-thermoelasticity, Figure 2 (first category) depicts the change in the distribution of the main physical variables under the impact of various relaxation times with increasing distance in the microelongated

semiconductor medium. In this group, real-dimensional numerical computations are performed in a relatively small amount of time, $t = 0.001$, while being influenced by laser pulses. As observed in the figure, the dual phase lag (DPL when $0 \leq \tau_\theta < \tau_q$) model is represented by the dashed line, while the dotted.

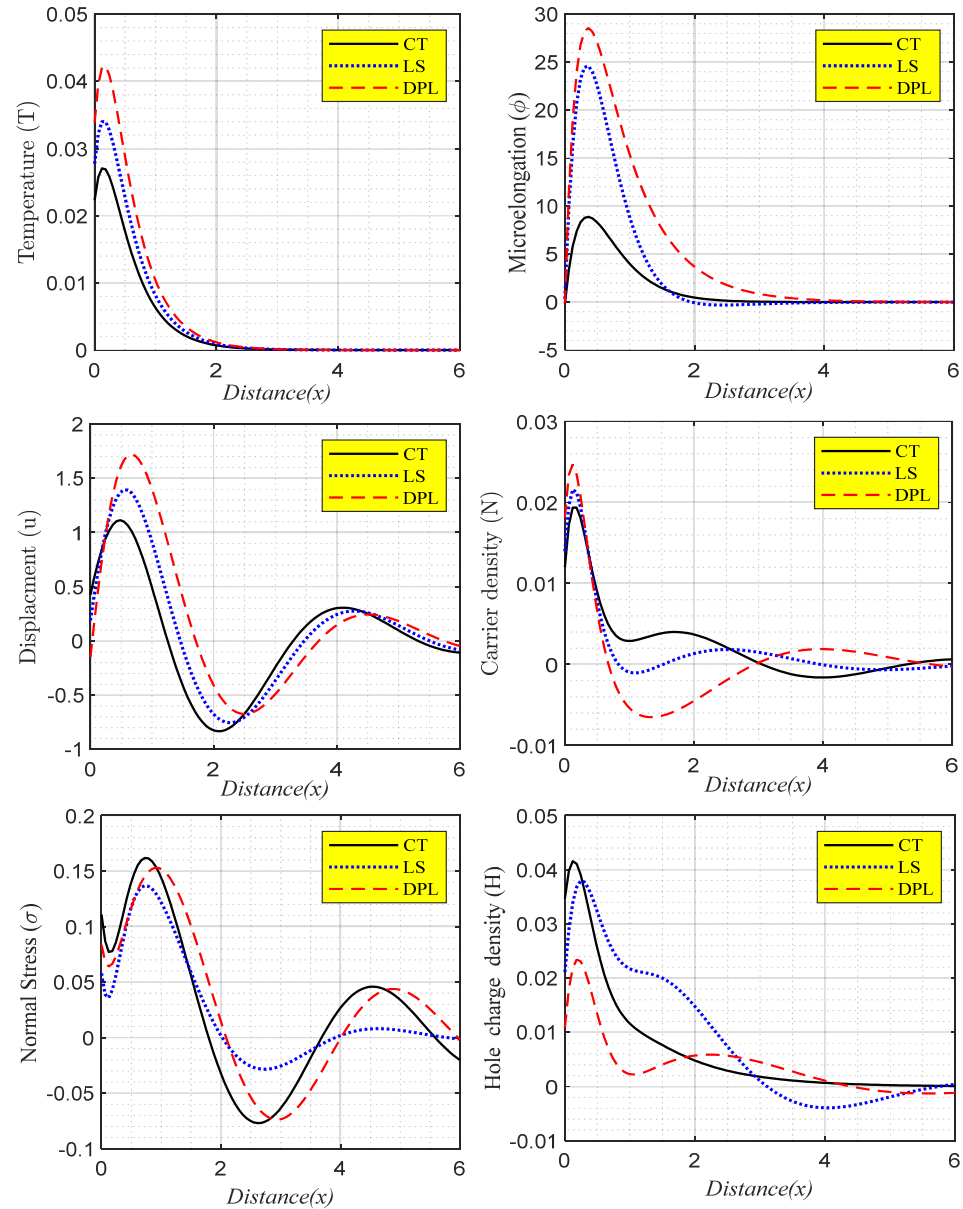


Figure 2. According to the two-temperature theory, the primary field distributions change with horizontal distance at various thermal memory (thermal relaxation durations) under the impact of laser pulses.

Line represents the Lord and Shulman (LS when $\tau_\theta = 0, 0 < \tau_q = 0.0002$) model, and the solid line represents the theory of coupled thermoelasticity (CT, when $\tau_\theta = \tau_q = 0.0$). The first subfigure depicts the thermal (heat) wave’s distribution, which is represented by the temperature distribution, where the distribution begins at the surface’s positive value and satisfies the boundary condition [48,49]. The numerical study showed that the structure’s maximum temperature consistently occurs close to the front of the heat wave and gradually decreases as the depth in the medium increases. The thermal wave distribution rises at the surface to achieve its maximum value as a direct consequence of the laser pulses’ influence, then progressively decreases, taking the form of an exponential

function. Further, under the surface, where the impact of the laser pulses is reduced, the distribution ultimately converges with the zero line to achieve the equilibrium state. These findings are consistent with what has been shown in actual experiments [50,51]. Microelongation wave propagation (the second subfigure), which begins at the surface from zero and increases in the closed initial range as a result of the action of laser pulses, may be used to characterize the microelongation scalar function. It then progressively diminishes with exponential behavior. The microelongation wave converges to the zero line far from the semiconductor surface because of the weak laser pulse effect until it reaches the equilibrium condition within the medium. The displacement distribution with increasing distance is used to indicate the shift in the elastic wave in the third subfigure. Due to the thermal impact of the laser pulses, the distribution begins at the surface nearing the zero value and progressively increases in the beginning to reach the highest value towards the edge. The distribution then alternately lowers and grows until it reaches its minimum value, just before it reaches an equilibrium state within the microelongated semiconductor medium. The increased collisions between the inner particles as a direct consequence of the heating action of the laser pulses cause this apparent perturbation in the elastic wave distribution. The fourth and sixth subfigures show the dispersion of plasma waves, which are represented by electron and hole diffusive activity with increasing distance (carrier density and hole charge density). In two cases, these distributions begin with positive values at the surface and satisfy the boundary surface conditions throughout the processes of recombination and replacement between them. When the temperature rise caused by the influence of laser pulses causes the diffusivity of electrons and holes to increase on the surface, they do so until they reach their maximum value. Moving further from the surface causes the distribution to progressively decrease until it achieves equilibrium in accordance with the zero line within the microelongated semiconductor medium, which is compatible with the experimental information and takes the shape of an exponential function [45,46]. On the other hand, the fifth subfigure depicts how the mechanical wave changes as the distance increases using normal stress distribution. The distribution starts out as a result of mechanical stress, which was applied at the surface from the positive value, satisfying the boundary condition and causing the distribution to smoothly decelerate in the initial range close to the edge. When the distribution reaches equilibrium within the semiconductor medium, it climbs gradually to achieve its maximum value before adopting a curve in the shape of wave distribution. The mechanical load and thermal impact of the laser pulses are both responsible for this apparent behavior in mechanical wave distribution. This results from the generation of mechanical forces and the operation of ultrafast lattice deformation.

7.2. The Laser Pulses Effect

The principal fields in this phenomenon vary depending on the different values of the laser pulses based on the power intensity (the pulse parameter p) versus a horizontal distance x , as shown in Figure 3 (second category). The numerical simulation is carried out during thermoelastic and electronic deformations over short moments, $t = 0.001$, under the influence of microelongation parameters, according to the DPL model. Two instances fall within this category: the first one is the disappearance of the laser pulse's influence (without the laser pulses effect), and the second one is the case of the laser pulses' effects (with the laser pulses effect). We investigated the impact of laser pulses on this model of equations, since it is evident that the thermal effect of laser pulses modifies the behavior of wave propagation in an obvious manner. From this, it is evident that the microelongated photothermal mechanical model, which accounts for all of these phenomena, can describe the ultrafast photothermal response to the laser pulse effect across the semiconductor medium.

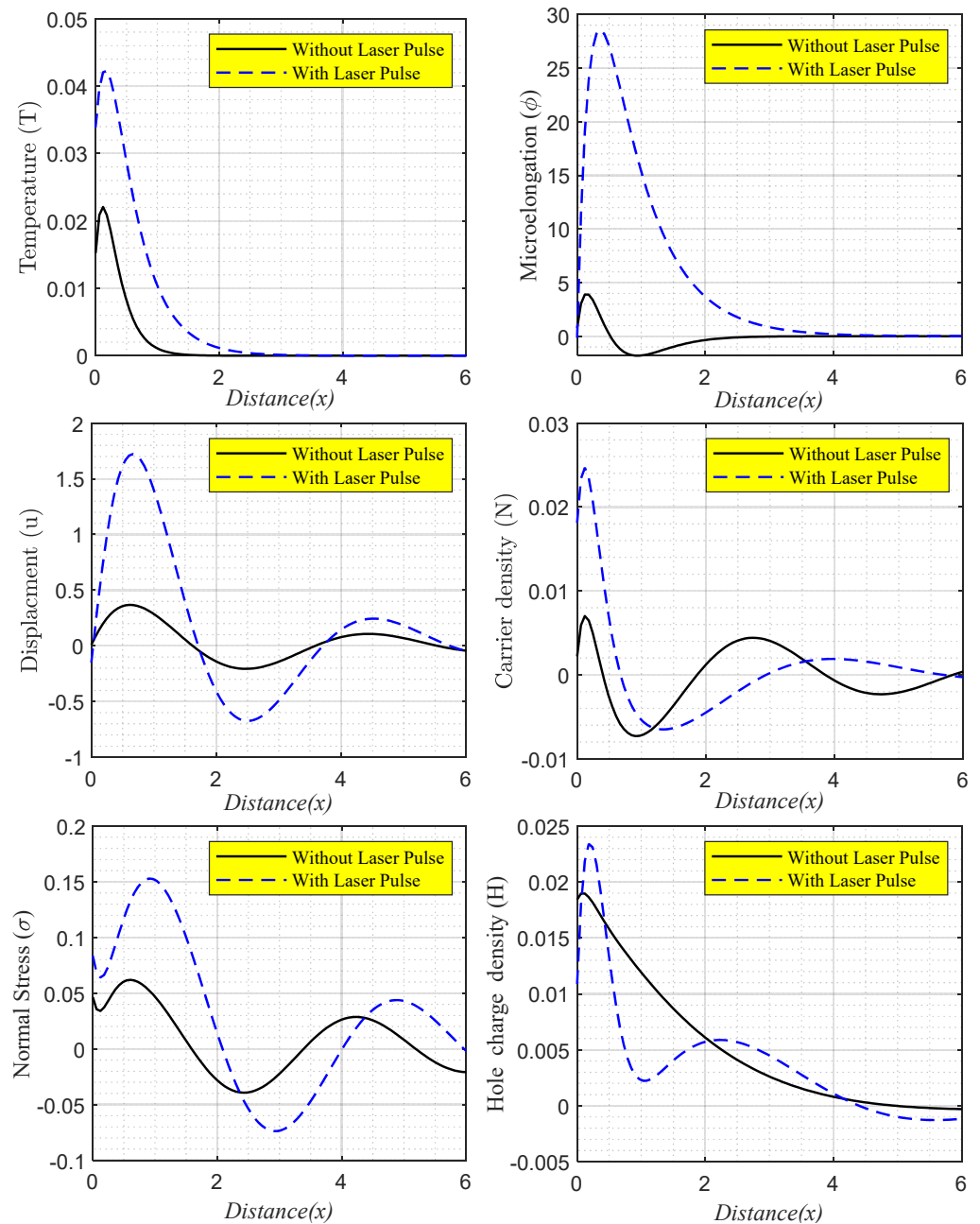


Figure 3. According to the DPL model, the main field distributions in two temperature fields under the impact of laser pulses and without them changing in terms of horizontal distance.

7.3. The Effect of Elongation Parameters

The third category (Figure 4) illustrates the variations in the main fields in this occurrence based on the different values of the microelongation parameters evaluated against the horizontal distance. The DPL model states that a numerical simulation is run during the brief electronic holes diffusion induced by laser pulses. Two instances fall within this category, the first of which is the loss of the microelongation parameters (without microelongation parameters when $\alpha_0 = \lambda_0 = \lambda_1 = 0$), and the second one is obtained when microelongation parameters are present. On the other hand, the behavior of wave propagation varies across all distributions. It is observed that the main field distribution behavior is greatly influenced by the microelongation parameters.

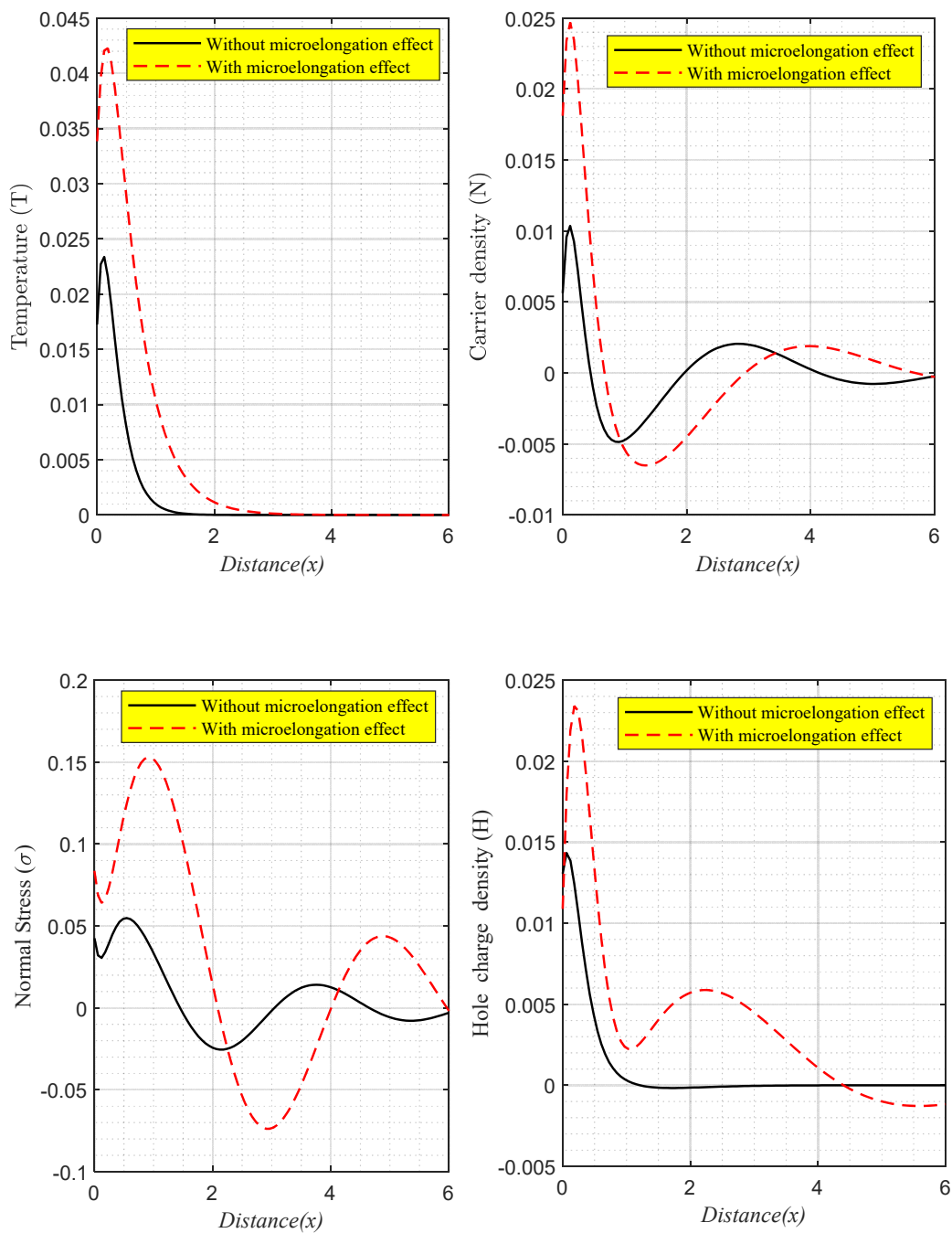


Figure 4. The main field distributions in distinct two temperature cases under the influence of laser pulses vary with horizontal distance in accordance with the DPL model.

8. Conclusions

In this study, we have presented the effects of mechanical loading, thermal memory, and extended photo-thermoelasticity on the properties of an n-type microelongated silicon semiconductor when it is subjected to laser pulses. The relationship between thermoelastic, microelongation, mechanical, and plasma waves is investigated when the material is photoexcited during an elasto-thermodiffusive process. The novel model is examined in the context of the microelongation effect during electronic holes diffusion. The difference between photo-thermoelasticity theories is taken into consideration based on thermal relaxation times. Thermal memory has a considerable influence on all of the main physical distribution wave propagations. However, all wave propagations are significantly influenced by the intensity of the laser pulses, as well as microelongation. A photo-thermoelastic

model was employed to forecast these variables, since the laser source had limitations in terms of its diameter and lifetime. An increasingly potent technique for assessing a material’s influence on its microstructure as a microelongated semiconductor is the generation of elastic waves as a consequence of brief thermal heating. The fact that these waves travel at rates of just a few kilometers per second is due to the extensive usage of semiconductors in the manufacturing of electronics and medical equipment. On the other hand, the direct possibility of creation, detection, and control being employed in the solar cell, as well as the energy of these waves being concentrated close to the top region of the device’s surface, make this sort of issue vital to research.

Author Contributions: Conceptualization, K.L.; Software, K.L.; Validation, K.L.; Formal analysis, I.M.T.; Investigation, I.M.T.; Data curation, A.A.E.-B. and J.A.; Writing—original draft, A.A.E.-B.; Writing—review & editing, J.A.; Visualization, M.A.Y.M.; Project administration, I.M.T.; All authors have read and agreed to the published version of the manuscript.

Funding: This research was funded by the Ministry of Education in Saudi Arabia through the project number (IFP-2022-47).

Data Availability Statement: The information applied in this research is available from the authors at request.

Acknowledgments: The authors extend their appreciation to the deputyship for research and innovation, the Ministry of Education in Saudi Arabia, for funding this research work through the project number (IFP-2022-47).

Conflicts of Interest: The authors have declared that no competing interests exist.

Nomenclature (The Physical Quantities with Units)

λ, μ	Elastic Lamé’s parameters.
$\delta_n = (3\lambda + 2\mu)d_n$	Deformation potential difference between conduction and valence band.
d_n	The electronic deformation coefficient ED
T_0	Reference temperature in its natural state
$\gamma = (3\lambda + 2\mu)\alpha_t$	Volume thermal expansion
σ_{ij}	Stress tensor
ρ	The density of the sample
α_t	Linear thermal expansion
p	The power intensity of the laser
C_e	Specific heat at constant strain
K	Thermal conductivity of the semiconductor medium
τ^n	The electrons relaxation time
τ_1^n	The lifetime of photogenerated carriers
E_g	Energy gap
e_{ij}	Components of the strain tensor
$m_{nq}, m_{qn}, m_{hq}, m_{qh}$	Peltier–Seebeck and Dufour–Soret-like constants
$a_{Qn}, a_{Qh}, a_Q, a_n, a_h$	The flux-like constants
τ_θ, τ_q	Thermal and elastic relaxation times
α_h, α_n	Holes and electrons thermo-diffusive parameters
n_0, h_0	The equilibrium value of electrons and holes concentration
$\delta_h = (2\mu + 3\lambda)d_h$	The holes elastodiffusive parameter
d_h	The coefficients of hole deformation
\tilde{s}	Recombination velocities
D_n, D_h	The diffusion coefficients of the electrons and holes
$a_0, \alpha_0, \lambda_0, \lambda_1$	Microelongational material parameters
m_k	Components of the microstretch vector
φ	The scalar microelongational function
$s = s_{kk}$	Stress tensor component

δ_{ik}	Kronecker delta
Ω	The pulse parameter
δ	The optical absorption coefficient

References

1. Chteoui, R.; Lotfy, K.; El-Bary, A.A.; Allan, M.M. Hall Current Effect of Magnetic-Optical-Elastic-Thermal-Diffusive Non-Local Semiconductor Model during Electrons-Holes Excitation Processes. *Crystals* **2022**, *12*, 1680. [[CrossRef](#)]
2. Saeed, A.M.; Lotfy, K.; Ahmed, M.H. Thermal-Optical Mechanical Waves of the Excited Microelongated Semiconductor Layer in a Rotational Field. *Mathematics* **2022**, *10*, 4660. [[CrossRef](#)]
3. Saeed, A.M.; Lotfy, K.; El-Bary, A.A. Hall Current Effect of Magnetic-Optical-Elastic-Thermal-Diffusive Semiconductor Model during Electrons-Holes Excitation Processes. *J. Math.* **2022**, *2022*, 6597924. [[CrossRef](#)]
4. Eringen, A.C.; Suhubi, E.S. Nonlinear theory of simple microelastic solids I. *Int. J. Eng. Sci.* **1964**, *2*, 189–203. [[CrossRef](#)]
5. Suhubi, E.S.; Eringen, A.C. Nonlinear theory of micro-elastic II. *Int. J. Eng. Sci.* **1964**, *2*, 389–404. [[CrossRef](#)]
6. Eringen, A.C. Linear theory of Micropolar Elasticity, ONR Technical Report No. 29. Ph.D. Thesis, School of Aeronautics, Aeronautics and Engineering Science, Purdue University, West Lafayette, IN, USA, 1965.
7. Eringen, A.C. A unified theory of thermomechanical materials. *Int. J. Eng. Sci.* **1966**, *4*, 179–202. [[CrossRef](#)]
8. Eringen, A.C. Linear theory of micropolar elasticity. *J. Math. Mech.* **1966**, *15*, 909–923.
9. Eringen, A.C. Micropolar elastic solids with stretch. *Ari Kitabevi Matbassi* **1971**, *24*, 1–18.
10. Youssef, H. Thermal shock problem of a generalized thermoelastic solid sphere affected by mechanical damage and thermal diffusion. *J. Eng. Therm. Sci.* **2021**, *1*, 1–16. [[CrossRef](#)]
11. Eringen, A.C. *Foundation of Micropolar Thermoelasticity, Courses and Lectures, No.23, CISM, Udine*; Springer: Vienna, Austria; New York, NY, USA, 1970.
12. Tauchert, T.R.; Claus, W.D.; Ariman, T. The linear theory of micropolar thermoelasticity. *Int. J. Eng. Sci.* **1968**, *6*, 37–47. [[CrossRef](#)]
13. Nowacki, W.; Olszak, W. Micropolar Thermoelasticity. In *Micropolar thermoelasticity, CISM Courses and Lectures, No. 151, Udine*; Nowacki, W., Olszak, W., Eds.; Springer: Vienna, Austria, 1974.
14. Lord, H.W.; Shulman, Y. A generalized dynamical theory of thermo-elasticity. *J. Mech. Phys. Solids* **1967**, *15*, 299–306. [[CrossRef](#)]
15. Müller, I.M. The coldness, a universal function in thermoelastic bodies. *Arch. Ration. Mech. Anal.* **1971**, *41*, 319–332. [[CrossRef](#)]
16. Green, A.E.; Laws, N. On the entropy production inequality. *Arch. Ration. Mech. Anal.* **1972**, *45*, 45–47. [[CrossRef](#)]
17. Green, A.E.; Lindsay, K.A. Thermoelasticity. *J. Elast.* **1972**, *2*, 1–7. [[CrossRef](#)]
18. Shaw, S.; Othman, M. On the concept of a conformable fractional differential equation. *J. Eng. Therm. Sci.* **2021**, *1*, 17–29. [[CrossRef](#)]
19. Lata, P.; Singh, S. Rayleigh wave propagation in a nonlocal isotropic magneto-thermoelastic solid with multi-dual-phase lag heat transfer. *GEM-Int. J. Geomath.* **2022**, *13*, 1869–2672. [[CrossRef](#)]
20. Kaur, I.; Lata, P.; Singh, K. Reflection of plane harmonic wave in rotating media with fractional order heat transfer and two temperature. *Partial. Differ. Equ. Appl. Math.* **2021**, *4*, 100049. [[CrossRef](#)]
21. Kaur, I.; Lata, P.; Singh, K. Reflection and refraction of plane wave in piezo-thermoelastic diffusive half spaces with three phase lag memory dependent derivative and two-temperature. *Waves Random Complex Media* **2022**, *32*, 2499–2532. [[CrossRef](#)]
22. Lata, P.; Singh, S. Effects of nonlocality and two temperature in a nonlocal thermoelastic solid due to ramp type heat source. *Arab. J. Basic Appl. Sci.* **2020**, *27*, 357–363. [[CrossRef](#)]
23. Kaur, I.; Lata, P.; Singh, K. Forced Flexural Vibrations in a Thin Nonlocal Rectangular Plate with Kirchhoff's Thin Plate Theory. *Int. J. Struct. Stab. Dyn.* **2020**, *20*, 1793–6764. [[CrossRef](#)]
24. Maruszewski, B. Electro-magneto-thermo-elasticity of Extrinsic Semiconductors, Classical Irreversible Thermodynamic Approach. *Arch. Mech.* **1986**, *38*, 71–82.
25. Maruszewski, B. Electro-magneto-thermo-elasticity of Extrinsic Semiconductors, Extended Irreversible Thermodynamic Approach. *Arch. Mech.* **1986**, *38*, 83–95.
26. Sharma, J.N.; Thakur, N.T. Plane harmonic elasto-thermodiffusive waves in semiconductor materials. *J. Mech. Mater. Struct.* **2006**, *1*, 813–835. [[CrossRef](#)]
27. Mandelis, A. *Photoacoustic and Thermal Wave Phenomena in Semiconductors*; Elsevier: New York, NY, USA, 1987.
28. Almond, D.; Patel, P. *Photothermal Science and Techniques*; Springer Science & Business Media: Berlin, Germany, 1996.
29. Gordon, J.P.; Leite, R.C.C.; Moore, R.S.; Porto, S.P.S.; Whinnery, J.R. Long-transient effects in lasers with inserted liquid samples. *Bull. Am. Phys. Soc.* **1964**, *119*, 501. [[CrossRef](#)]
30. Lotfy, K. Effect of Variable Thermal Conductivity during the Photothermal Diffusion Process of Semiconductor Medium. *Silicon* **2019**, *11*, 1863–1873. [[CrossRef](#)]
31. Lotfy, K.; Abo-Dahab, S.; Tantawy, R.; Anwar, N. Thermomechanical Response Model on a Reflection Photothermal Diffusion Waves (RPTD) for Semiconductor Medium. *Silicon* **2020**, *12*, 199–209. [[CrossRef](#)]
32. Alharbi, A.R.; Almatrafi, M.B.; Lotfy, K. Constructions of solitary travelling wave solutions for Ito integro-differential equation arising in plasma physics. *Results Phys.* **2020**, *19*, 103533. [[CrossRef](#)]
33. Lotfy, K. A novel model of magneto photothermal diffusion (MPD) on polymer nano-composite semiconductor with initial stress. *Waves Ran. Comp. Med.* **2021**, *31*, 83–100. [[CrossRef](#)]

34. Lotfy, K.; Elidy, E.S.; Tantawi, R. Piezo-photo-thermoelasticity transport process for hyperbolic two-temperature theory of semiconductor material. *Int. J. Mod. Phys. C* **2021**, *32*, 2150088. [[CrossRef](#)]
35. Mahdy, A.M.S.; Lotfy, K.; El-Bary, A.; Tayel, I.M. Variable thermal conductivity and hyperbolic two-temperature theory during magneto-photothermal theory of semiconductor induced by laser pulses. *Eur. Phys. J. Plus* **2021**, *136*, 651. [[CrossRef](#)]
36. Abbas, I.; Hobiny, A. Analytical-numerical solutions of photo-thermal interactions in semiconductor materials. *Inf. Sci. Lett.* **2021**, *10*, 189–196.
37. Abbas, I.A.; Alzahrani, F.S.; Elaiw, A. A DPL model of photothermal interaction in a semiconductor material. *Waves Random Complex Media* **2019**, *29*, 328–343. [[CrossRef](#)]
38. Khamis, A.K.; Lotfy, K.; El-Bary, A.A.; Mahdy, A.M.S.; Ahmed, M.H. Thermal-piezoelectric problem of a semiconductor medium during photo-thermal excitation. *Waves Random Complex Media* **2021**, *31*, 2499–2513. [[CrossRef](#)]
39. Mahdy, A.; Lotfy, K.; Ismail, E.; El-Bary, A.; Ahmed, M.; El-Dahdouh, A. Analytical solutions of time-fractional heat order for a magneto-photothermal semiconductor medium with Thomson effects and initial stress. *Results Phys.* **2020**, *18*, 103174. [[CrossRef](#)]
40. Mahdy, A.M.S.; Lotfy, K.; Hassan, W.; El-Bary, A.A. Analytical solution of magneto-photothermal theory during variable thermal conductivity of a semiconductor material due to pulse heat flux and volumetric heat source. *Waves Random Complex Media* **2021**, *31*, 2040–2057. [[CrossRef](#)]
41. Lotfy, K. The elastic wave motions for a photothermal medium of a dual-phase-lag model with an internal heat source and gravitational field. *Can. J. Phys.* **2016**, *94*, 400–409. [[CrossRef](#)]
42. Marin, M. A domain of influence theorem for microstretch elastic materials. *Nonlinear Anal. Real World Appl.* **2010**, *11*, 3446–3452. [[CrossRef](#)]
43. Marin, M. A partition of energy in thermoelasticity of microstretch bodies. *Nonlinear Anal. Real World Appl.* **2010**, *11*, 2436–2447. [[CrossRef](#)]
44. Brancik, L. Programs for fast numerical inversion of Laplace transforms in MATLAB language environment. In Proceedings of the 7th Conference MATLAB, Brno, Czech Republic, January 1999.
45. Mahdy, A.M.S.; Lotfy, K.; El-Bary, A.; Sarhan, H.H. Effect of rotation and magnetic field on a numerical-refined heat conduction in a semiconductor medium during photo-excitation processes. *Eur. Phys. J. Plus* **2021**, *136*, 553. [[CrossRef](#)]
46. Lotfy, K. A novel model for Photothermal excitation of variable thermal conductivity semiconductor elastic medium subjected to mechanical ramp type with two-temperature theory and magnetic field. *Sci. Rep.* **2019**, *9*, 3319. [[CrossRef](#)]
47. Mondal, S.; Sur, A. Photo-thermo-elastic wave propagation in an orthotropic semiconductor with a spherical cavity and memory responses. *Waves Random Complex Media* **2020**, *31*, 1835–1858. [[CrossRef](#)]
48. Aldwoah, K.A.; Lotfy, K.; Mhemdi, A.; El-Bary, A. A novel magneto-photo-elasto-thermodiffusion electrons-holes model of excited semiconductor. *Case Stud. Therm. Eng.* **2022**, *32*, 101877. [[CrossRef](#)]
49. Alhejaili, W.; Lotfy, K.; El-Bary, A. Photo-elasto-thermodiffusion waves of semiconductor with ramp-type heating for electrons-holes-coupled model with initial stress. *Waves Random Complex Media* **2022**, *22*, 1–9. [[CrossRef](#)]
50. Xiao, Y.; Shen, C.; Zhang, W.B. Screening and prediction of metal-doped α -borophene monolayer for nitric oxide elimination. *Mater. Today Chem.* **2022**, *25*, 100958. [[CrossRef](#)]
51. Liu, J.; Han, M.; Wang, R.; Xu, S.; Wang, X. Photothermal phenomenon: Extended ideas for thermophysical properties characterization. *J. Appl. Phys.* **2022**, *131*, 065107. [[CrossRef](#)]

Disclaimer/Publisher’s Note: The statements, opinions and data contained in all publications are solely those of the individual author(s) and contributor(s) and not of MDPI and/or the editor(s). MDPI and/or the editor(s) disclaim responsibility for any injury to people or property resulting from any ideas, methods, instructions or products referred to in the content.